WSRC-TR-2001-00212

Cross-Flow Filtration Demonstration for Slurries Containing High Level Waste Sludge and Monosodium Titanate

M. R. Poirier, F. F. Fondeur, T. L. Fellinger, and S. D. Fink
Westinghouse Savannah River Company
Aiken, SC 29808

This document was prepared in conjunction with work accomplished under Contract No. DE-AC09-96SR18500 with the U.S. Department of Energy.

DISCLAIMER

This report was prepared as an account of work sponsored by an agency of the United States Government. Neither the United States Government nor any agency thereof, nor any of their employees, makes any warranty, express or implied, or assumes any legal liability or responsibility for the accuracy, completeness, or usefulness of any information, apparatus, product or process disclosed, or represents that its use would not infringe privately owned rights. Reference herein to any specific commercial product, process or service by trade name, trademark, manufacturer, or otherwise does not necessarily constitute or imply its endorsement, recommendation, or favoring by the United States Government or any agency thereof. The views and opinions of authors expressed herein do not necessarily state or reflect those of the United States Government or any agency thereof.

This report has been reproduced directly from the best available copy.

Available for sale to the public, in paper, from: U.S. Department of Commerce, National Technical Information Service, 5285 Port Royal Road, Springfield, VA 22161, phone: (800) 553-6847, fax: (703) 605-6900, email: orders@ntis.fedworld.gov online ordering: http://www.ntis.gov/support/ordering.htm

Available electronically at http://www.osti.gov/bridge/

Available for a processing fee to U.S. Department of Energy and its contractors, in paper, from: U.S. Department of Energy, Office of Scientific and Technical Information, P.O. Box 62, Oak Ridge, TN 37831-0062, phone: (865) 576-8401, fax: (865) 576-5728, email: reports@adonis.osti.gov

Keyword: Salt Waste Processing Facility (SWPF), Filtration, Sludge

Abbreviations

ADS	Analytical Development Section
CST	Crystalline silicotitanate
CUF	Cells Unit Filter
DSC	Differential scanning calorimetry
FRED	Filtration Research Engineering Demonstration facility located at the University of South Carolina
ICP-ES	Inductively-coupled plasma emissions spectroscopy
ICP-MS	Inductively-coupled plasma mass spectroscopy
JMPâ	Statistical software package manufactured by SAS Institute, Inc., Cary, NC, version 4.0 ã 2000
MST	Monosodium titanate
PREF	Parallel Rheology Experimental Filter

SRS	Savannah River Site
SRTC	Savannah River Technology Center
TMP	Transmembrane pressure

Summary

The authors performed cross-flow filtration tests using supernatant (5.6M [Na]) from Tanks 37H and 44H, MST, and sludge from any of three waste tanks (Tanks 51H, 11H, and 8F). The tests occurred in the SRTC Shielded Cells using the Cells Unit Filter (CUF). The experiments varied the axial velocity and transmembrane pressure in a statistically designed matrix to mimic conditions in previous cross-flow filtration tests performed with simulated waste using the Parallel Rheology Experimental Filter and the Filtration Research Engineering Demonstration. The insoluble solids concentration varied between 0.06 wt % and 6.0 wt %. The authors also conducted differential scanning calorimetry (DSC) and rheology tests on concentrated sludge and MST samples. Testing yielded the following conclusions.

- The filter flux for the real waste shows a positive bias relative to predictions based upon tests with simulated waste. The variance remains within the statistical accuracy of the predictive correlation except for slurries with the highest concentration of solids tested (i.e., 6.0 wt %)
- The simulated sludge used in previous cross flow filtration testing serves as a reasonable representative of actual Savannah River Site sludge. Data from these tests provide a conservative estimate of equipment size and required operating conditions.
- We observed no significant difference in the filtration rates with Tank 51H sludge and Tank 8F sludge.
- Feed solutions prepared with dried sludge had higher filtration rates than feed solutions prepared with slurry sludge. Only a limited number of waste tanks contain dried sludge. Hence, the authors recommending using the behavior of the slurry samples as more representative of expected behavior for the process.
- The concentrated sludge and the sludge plus MST slurries (6.0 wt % insoluble solids) had yield stresses less than 3.5 Pa. The data agreed well with previous data where available.

Introduction

The Salt Disposition Systems Engineering Team selected three cesium removal technologies for further development to replace the In Tank Precipitation process: Small Tank Tetraphenylborate Precipitation, Non-elutable Ion Exchange using crystalline silicotitanate as the sorbent, and Caustic-Side Solvent Extraction.

As a pretreatment step for the CST and solvent extraction flowsheets, the operation contacts the incoming salt solution containing entrained sludge with monosodium titanate to adsorb strontium, plutonium, and other actinides. The process then filters the resulting slurry to remove the sludge and MST. Cesium removal occurs by contacting the filtrate with CST in an ion exchange column or processing through a solvent extraction system. Testing performed by SRTC and the University of South Carolina with simulated waste demonstrated filtration rates of 0.03 – 0.08 gpm/ft^2. ' A systems engineering study identified one technology risk as whether the sludge used to prepared the simulated waste for filtration testing adequately represents SRS waste. Because of this risk, High Level Waste Process Engineering requested SRTC to conduct cross-flow filter tests with real waste.

Experimental

The authors conducted cross-flow filtration tests using a 0.5 m pore size, 3/8" ID Mott cross-flow filter in the SRTC Shielded Cells. The feed for the tests contained SRS High Level Waste supernatant, SRS High Level Waste sludge, and Aqua Air MST. The tests used a solution concentration of 5.6 M sodium and an insoluble solids loading of 0.06 – 6.0 wt %. The testing varied the axial velocity and transmembrane pressure (TMP) to repeat test conditions used previously at the Filtration Research Engineering Demonstration (FRED) and with the Parallel Rheology Experimental

Filter (PREF).

Cross-flow Filtration Equipment

Figure 1 shows the Cells Unit Filter (CUF) used to perform these tests. The equipment contains a sintered stainless steel 0.5 m pore-size Mott cross-flow filter of 3/8" inner diameter and 2-ft length. The filtration unit contains a feed vessel, a feed pump, a heat exchanger to control solution temperature, a magnetic flow meter to measure the filter feed rate, and three calibrated pressure gauges to measure feed, concentrate, and filtrate pressure. A graduated glass cylinder located down stream of the filter allows measurement of flux. Personnel determined the filtrate flow rate, or flux, by measuring the time to collect a known volume of filtrate. The working volume of the equipment measures approximately 800 mL.

Personnel have used the equipment previously to evaluate cross-flow performance with actual radioactive waste from the Savannah River Site and the Hanford Site.

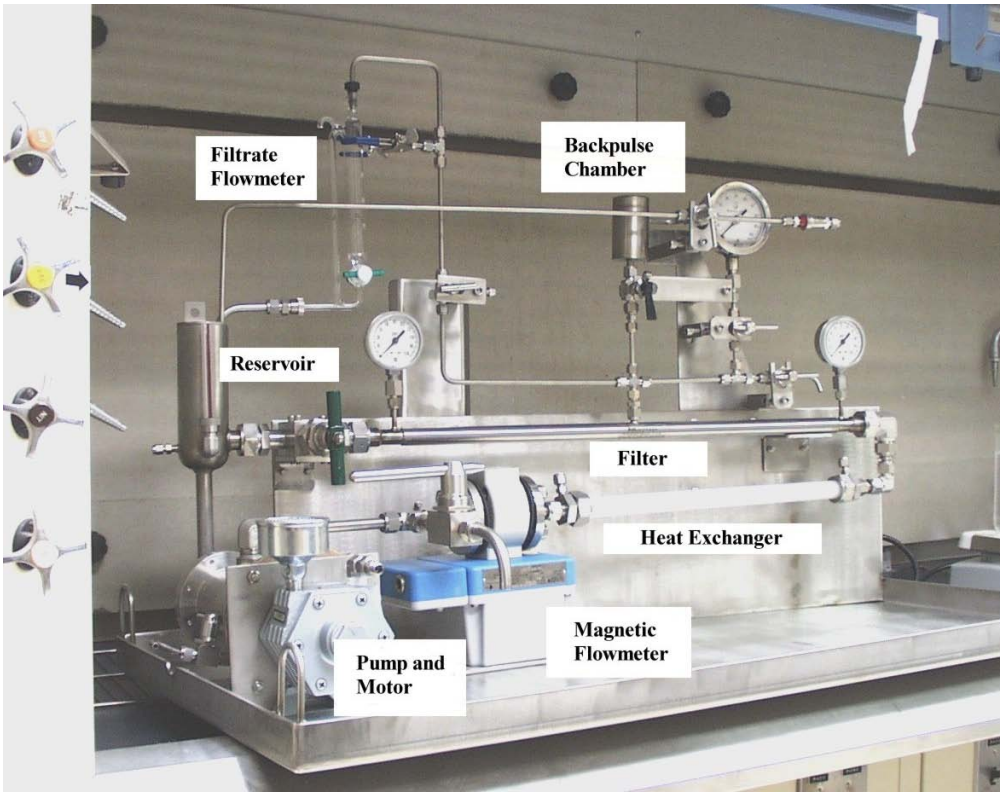

Figure 1. Filter Equipment Shown Prior to Installation in Shielded Cell

Experimental Approach – Actual High Level Waste

We obtained samples of SRS High Level Waste supernatant collected in September 2000 and received in the SRTC Shielded Cells on October 1, 2000. The solution came from Tanks 37H and 44H. The authors also obtained SRS High Level Waste sludge from samples archived previously at SRTC and samples delivered shortly before the current test. The sludge samples came from the Tank 51H, Tank 8F, and Tank 11H. The Tank 8F sludge came from slurry, the Tank 11H sludge came from a dried sample and the Tank 51H sludge came from either a slurry or dried sample.

Personnel prepared the first supernatant sample by blending 400 mL of Tank 37F/44H supernatant with 600 mL of 2 M NaOH, and mixing by shaking with the manipulator for 15 minutes. We measured the solution density by weighing an empty 100 mL calibrated graduate cylinder, adding a known volume of solution to the graduate cylinder, and measuring the mass. The density of this solution measured 1.227 g/mL.

We collected a sample of this solution, diluted it to reduce the radiation level, and submitted it to ADS for sodium

analysis. The sodium concentration measured 4.7 M by AA and 6.2 M by ICP-ES. After reviewing the results with Doug Walker who had also used this material in other tests, reviewing the ADS analytical procedures, and considering the measured solution density, we accepted the concentration of sodium to be 6.2 M. We then added 167 mL of 2 M NaOH to the solution to reduce the sodium concentration to 5.6 M Na. We prepared additional samples by mixing 274 mL of Tank 37F/44H solution with 528 mL of 2M NaOH.

Table 1 shows the target insoluble solids concentration for each test. Personnel prepared the feed for the first test by taking the solution sample and adding sludge (Tank 51H) to bring the concentration to 0.06 wt % insoluble solids. They mixed the feed and processed it through the cross-flow filter. The testing varied the axial velocity and TMP for comparison with previous filter test data.[1,2,5] As in the earlier reference study, experiments followed a statistically designed matrix. Table 2 shows the target axial velocity and TMP for the tests. Personnel combined additional sludge (Tank 51H) with the slurry to bring the concentration to 0.29 wt % insoluble solids and measured filter performance. Following the filtration test, personnel again increased the insoluble solids concentration to 1.29 wt %. A final filter test occurred with 6.0 wt % insoluble solids. The solids levels were selected to repeat conditions tested at FRED.

Table 1. Targeted Insoluble Solids Concentration for Real Waste Filter Tests

Tank 51H	Tank /8F	Tank 11H*	Tank 51H*	FRED Feed
0.031 wt % sludge 0.029 wt % MST	0.031 wt % sludge 0.029 wt % MST	0.031 wt % sludge 0.029 wt % MST	0.06 wt % sludge	N/A
0.15 wt % sludge 0.14 wt % MST	0.15 wt % sludge 0.14 wt % MST	0.15 wt % sludge 0.14 wt % MST	0.29 wt %sludge	N/A
0.67 wt % sludge 0.62 wt % MST	0.67 wt % sludge 0.62 wt % MST	0.67 wt % sludge 0.62 wt % MST	1.29 wt % sludge	N/A
3.1 wt % sludge 2.9 wt % MST	3.1 wt % sludge 2.9 wt % MST	3.1 wt % sludge 2.9 wt % MST	6.0 wt % sludge	4.7 wt % Tank 8 Simulated Sludge
**** These experiments used a previously dry sample of sludge from the respective tanks.***				

Table 2. Target Axial Velocity and Transmembrane Pressure

0.06, 0.29, and1.19 wt % (nominal) Insoluble Solids		6.0 wt % (nominal) Insoluble Solids	
Axial Velocity (ft/s)	TMP (psi)	Axial Velocity (ft/s)	TMP (psi)
6	15	6	30
6	41	6	41
12	15	12	30
12	41	12	41
9	28	9	36
9	28	9	36

Personnel repeated this procedure for the Tank 51H sludge, the Tank 8F sludge, and the Tank 11H sludge. In these tests, the insoluble solids included both sludge and MST. A final test used 4.7 wt % Tank 8F simulated sludge, obtained from personnel at the University of South Carolina, to allow a direct comparison of performance between the

CUF and the FRED facility.

The MST (AuqaAir) initially had a mean particle size of 7.3 m, 12.26% of particles larger than 44 m, and 1.29% of particles less than 0.972 m. Since this material did not meet the HLW specification for MST, personnel crushed the material in a grinder. The resulting slurry had a mean particle size of 5.3 m, 2.76% of the particles larger than 44 m, and 1.66% of the particles less than 0.972 m. The treated material still failed to meet specifications but did contain significantly less large particles. We wanted to avoid the large particles to avoid positively biasing the measured filter flux.

Prior to the test at each operating condition, researchers backpulsed the filter to remove solids that had accumulated on the filter surface during previous tests.

Prior to performing tests with a new feed solution, personnel cleaned the filter with 0.5 M nitric acid or 0.5 M oxalic acid.

Prior to the addition of sludge or MST, we measured the density of each solution.

During the tests, personnel collected solution samples for sodium and anion analyses. If the feed solution contained no insoluble solids, we collected the sample from the feed vessel. If the feed solution contained insoluble solids, we pulled the sample from the filtrate sample valve to the right of the filtrate pressure gauge on the CUF.

Researchers collected samples to measure insoluble solids content during the tests by circulating the feed solution and collecting a sample from the feed-side sample valve upstream of the magnetic flow meter.

At the end of the tests with each feed solution, personnel collected samples for differential scanning calorimetry (DSC), rheology determination, and particle size analysis. The samples collected for particle size analysis had radiation levels too high to allow for removal from the cells and particle size analysis by Microtrac. The authors continue to evaluate other methods to measure particle size of the sludge in these tests.

Thermal Analyses

The Differential Scanning Calorimetry (DSC) analyses occurred in the following manner. Personnel took between 20 to 50 mg of liquid sample and placed it in a stainless steel cup. They then sealed the cup with a Viton™ o-ring and placed it in a 550E Differential Scanning Calorimeter from ISI (Instrument Specialist Incorporated). The DSC calculates the heat given off or taken in by the solution by measuring the temperature difference between the sample and a reference sample. We used an empty stainless steel cup as a reference. Personnel preheated the samples to 40 ° C for 10 minutes to reduce any gas super saturation in the solution. After cooling, personnel then heated the sample from 15 ° C to 100 ° C at 10 ° C/min and weighed after the DSC measurements to determine a mass loss.

Rheology Measurements

Personnel measured the rheological properties of six radioactive samples containing sludge from Tank 51H, Tank 8F, and Tank 11H with a Haake RV30/M5 system. The Haake RV30/M5 system is a controlled rate rheometer that can operate remotely in the Shielded Cells environment. A water-bath/circulator uses water to maintain the temperature of the water jacket that surrounds the sample cup. Measurements occurred at 25 ° C. The M5 measuring head can use different sample cups and rotors depending on the type of fluid analyzed. Some of the samples contained only sludge, while other samples contained sludge and MST.

The solids present in the samples suspended easily upon shaking, and did not appear to settle quickly. For this reason, we selected the MV1 ("medium viscosity 1") rotor and used this configuration for all of the flow measurements. Personnel typically use the MV1 rotor for fluids working in the medium shear rate range. We used a Newtonian oil standard (95.6 cp @ 25° C) to check the instrument’s response prior to the start of the measurements and at the end of the last measurement. The oil standard check ensured that the instrument responded as expected. Appendix 2 contains additional detail related to the equipment and the control standard.

Results and Discussion

Demonstration using SRS High-Level Waste

Figure 2 through Figure 5 show comparisons between the filter flux in the current test and that measured in previous engineering-scale filtration tests performed at the FRED facility. The separate plots display filter flux (in gpm/ft^2) plotted against the transmembrane pressure (TMP) at each concentration of insoluble solids. The concentrations in the figure titles are the target concentrations or the test. In the most recent tests at FRED, the flux depended strongly on TMP and concentration, with much less influence from axial velocity. The filter flux measured with actual SRS waste in this test equals or exceeds the flux measured with simulated waste at FRED. The filter flux with the simulated Tank 8F sludge slurry (from FRED) also proved significantly higher in the CUF than in the FRED facility.

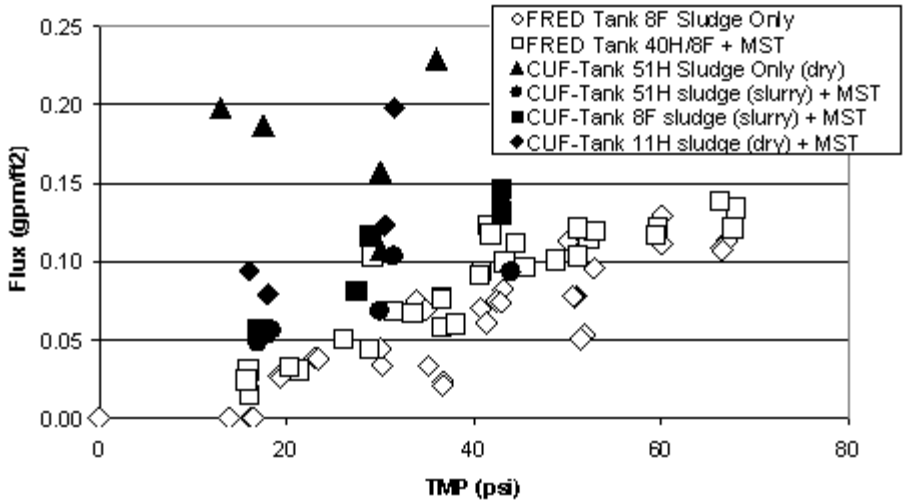

Figure 2. Comparison of Cross-flow Filter Flux between FRED and CUF with 0.06 wt % (nominal) Insoluble Solids

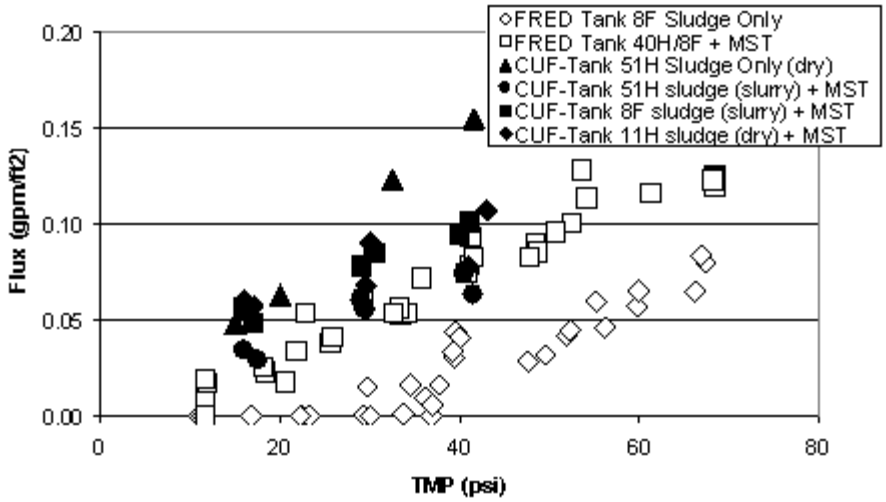

Figure 3. Comparison of Cross-flow Filter Flux between FRED and CUF with 0.29 wt % (nominal) Insoluble Solids

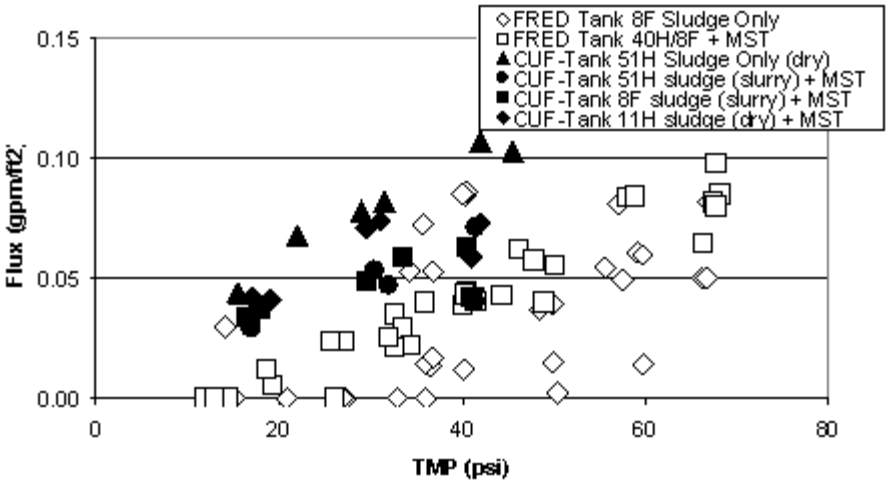

Figure 4. Comparison of Cross-flow Filter Flux between FRED and CUF with 1.13 wt % (nominal) Insoluble Solids

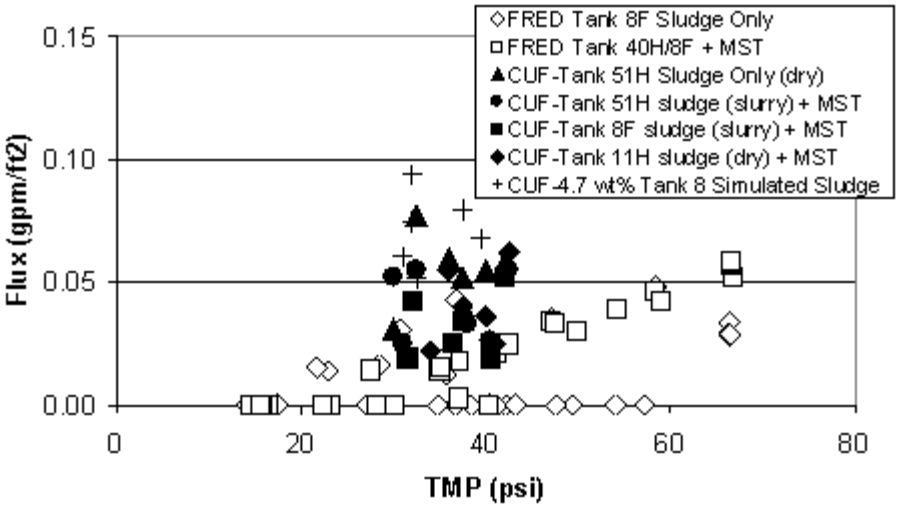

Figure 5. Comparison of Cross-flow Filter Flux between FRED and CUF with 6.0 wt % (nominal) Insoluble Solids

Many of the flux measurements in the tests performed with either the Tank 51H sludge slurry or the combined MST and Tank 11H sludge slurry proved higher than the flux in other tests. Both samples used sludge from a dry archived sample. The flux values remained high for all the experiments using the slurry containing Tank 51H sludge. The discrepancy seemed less apparent in the tests using slurry containing MST and Tank 11H sludge as the MST concentration increased. The authors believe the higher flux values resulted from larger solid aggregates in the slurries containing previously dry sludge. The technicians preparing the samples reported large aggregates and noted that grinding only seemed to marginally reduce particle sizes when compared against slurries containing previously wet sludge. In the case of the Tank 11H material, perhaps as the MST concentration increased, these solids helped abrade the sludge aggregates and reduced mean particle sizes. Alternatively, the MST solids simply reduced the mean particle size by diluting the average particle properties. Also, the presence of MST likely increased the particle size variability in the feed solution. The increased particle size variability would allow the solids to pack more tightly in a filter cake and reduce the filter flux. The experiment using the slurry containing only Tank 51H sludge solids also represented the first test with a new filter element. Flux measurements for a new filter element always prove higher than that for a cleaned filter, but past experience shows a minimal offset as the testing proceeds.

The filter flux with slurries containing real SRS High Level Waste sludge and supernatant proved higher than the filter

flux measured with simulant during engineering-scale filtration testing performed at FRED in FY00 and FY01." Since the various tests contain three independent variables (axial velocity, insoluble solids concentration, and transmembrane pressure), one can not readily compare two sets of data on a single graph. Another approach for comparing data sets uses the cross-flow filtration model developed in FY00 and described by equation 1.

$$\begin{aligned} \text{Flux(gpm/ft}^2) = \; & 0.0147 + 0.00186 \times \text{TMP (psi)} \\ & - 0.0192 \times \ln(\text{concentration(g/L)}) \\ & - 0.000035 \times (\text{axial velocity (ft/s)}^{1.5}) / \text{concentration(g/L)}^2 \end{aligned} \quad [1]$$

Using the operating parameters from the current test (axial velocity, insoluble solids concentration, and transmembrane pressure), one can predict the filter flux for each of the experiments performed and compare that value with the measured filter flux. The model described by equation 1 tends to over-predict the filter flux for these tests. Equation 1 derived from data collected during tests with an axial velocity between 12 and 26 ft/s. The axial velocity in the current tests ranged from 6 to 12 ft/s.

The authors refined the model using all the available data from engineering-scale tests performed at FRED. During the FY98 tests, the axial velocity varied between 4 ft/s and 14 ft/s. We analyzed the data from both sets of tests with the JMPâ software and developed equation 2.

$$\begin{aligned} \text{Flux(gpm/ft}^2) = \; & 0.0201 + 0.00162 \times \text{TMP (psi)} \\ & - 0.0160 \times \ln(\text{concentration (g/L)}) \\ & - 0.000096 \times (\text{axial velocity (ft/s)}^{1.5}) / \text{concentration(g/L)}^2 \end{aligned} \quad [2]$$

After comparing the data from the FY98 and FY00 tests with the model described by equation 2, the authors calculated a standard deviation for the data from each test set relative to the model. The standard deviation of the data from the FY00 test equals 21%, and the standard deviation of the data from the FY98 test equals 27%.

The data from which equation 2 derived used axial velocities between 4 ft/s and 26 ft/s. The majority of the data came from an axial velocity greater than 10 ft/s. The authors calculated the residual (difference between predicted flux and measured flux) and plotted it as a function of axial velocity in Figure 6. The figure also shows the axial velocity range from the present test. The residuals have the largest magnitude at axial velocities between 9 and 14 ft/s, which overlaps the axial velocity used in the current tests (6 – 12 ft/s).

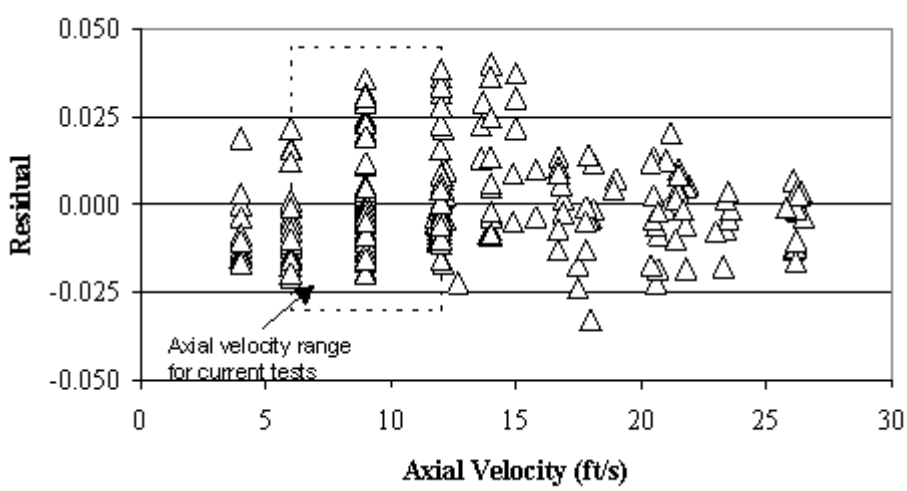

Figure 6. Residual as a Function of Axial Velocity from Model Described by Equation 2

Figure 7 shows the ratio of the predicted filter flux to the measured filter flux from the data points used to develop

equation 2. This plots shows the model predicts cross-flow filter flux best at axial velocities of 20 – 26 ft/s.

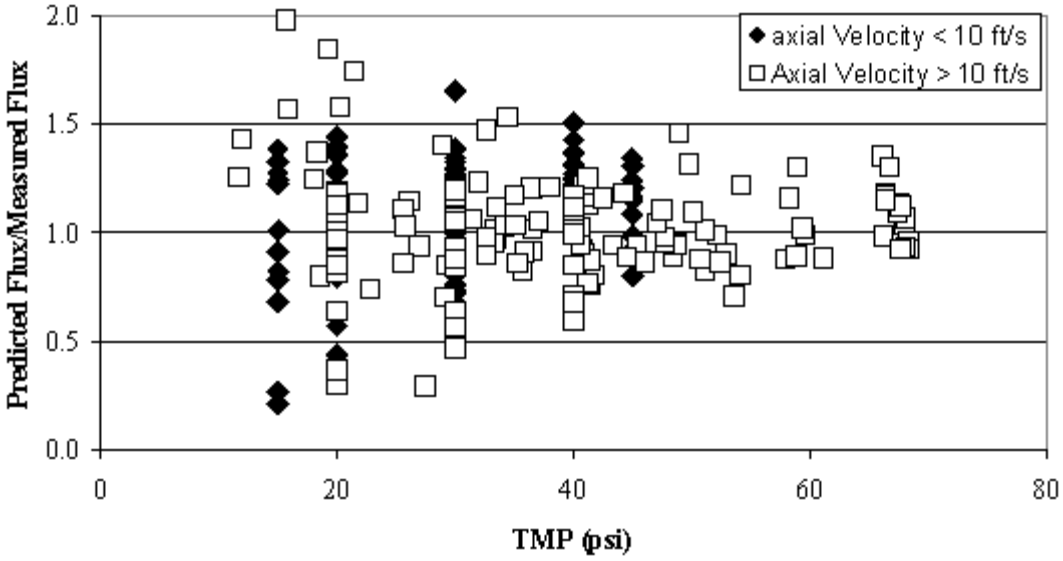

Figure 7. Comparison between Predicted Flux and Measured Flux for Data Used to Develop Equation 2

Using equation 2, we then calculated the ratio of predicted flux to measured flux and plotted it as a function of transmembrane pressure in Figure 8 through Figure 11 (measured concentration used to predict filter flux). The plots compare measured flux at a given concentration of insoluble solids to the predicted values (concentration in figure title is target concentration). The plots also contain lines showing ± 2 standard deviations (± 54%). In general, the measured flux exceeds that based on the prediction. At the three lowest insoluble solids levels, the measured flux from the current test falls within 2 standard deviations of the predicted flux. At the highest insoluble solids concentration, the agreement between measured filter flux and predicted filter flux proves worse.

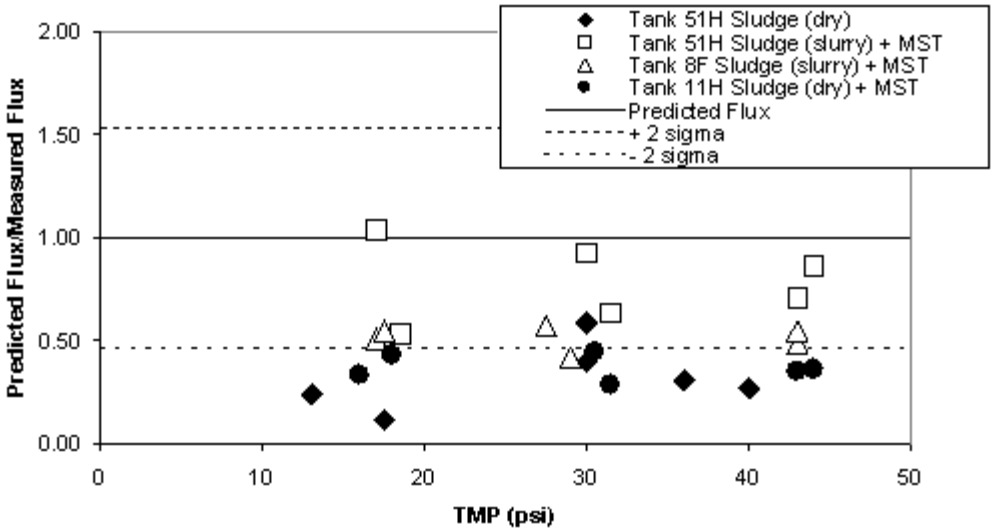

Figure 8. Comparison between Predicted Flux and Measured Flux at 0.06 wt % Insoluble Solids

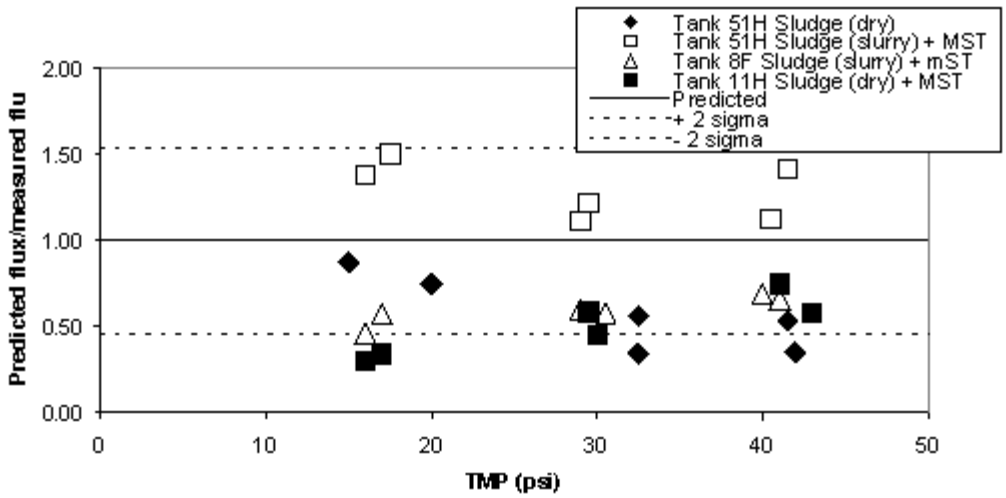

Figure 9. Comparison between Predicted Flux and Measured Flux at 0.29 wt % Insoluble Solids

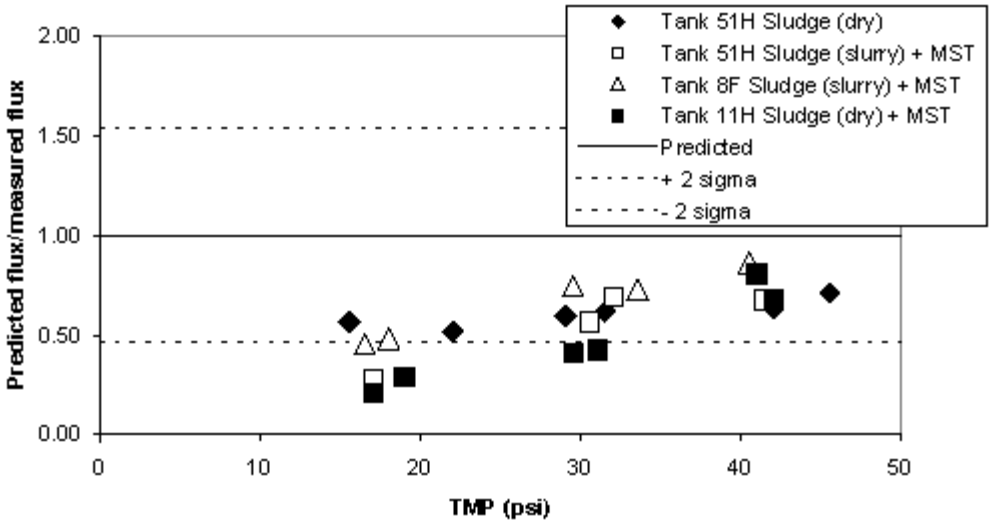

Figure 10. Comparison between Predicted Flux and Measured Flux at 1.19 wt % Insoluble Solids

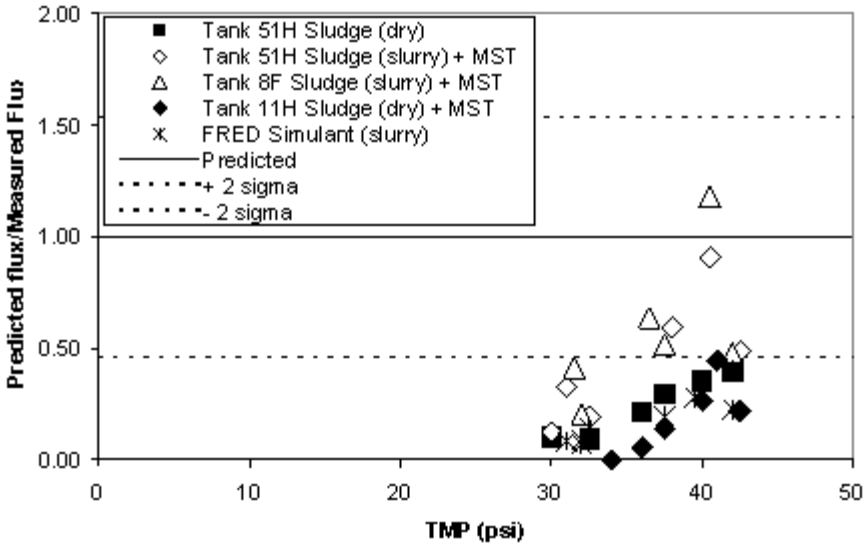

Figure 11. Comparison between Predicted Flux and Measured Flux at 6.0 wt % Insoluble Solids

In theses figures, the open symbols correspond to feed solutions prepared with wet sludge, and the closed symbols correspond to feed solutions prepared with dried sludge. In general, the flux from tests with feeds prepared from wet sludge more closely match predictions than the flux from tests with feeds prepared from dried sludge. Figure 9 provides a good example of this difference. In that figure the average predicted flux/measured flux for feed solutions prepared with slurry sludge equals 0.94. The average for feed solutions prepared with previously dry sludge equals 0.54.

The goodness of fit – or degree of agreement between measured and predicted values – also appears to vary with concentration of solids and with TMP. As the concentration of solids increases, the agreement decreases with the experimentally determined flux from the real waste proving higher than that predicted from equation 2. Similarly, within a data set for a given concentration of solids, the agreement becomes better at increased TMP. Recall that the data set used to develop equation 2 included more information at higher TMP and higher axial velocity. Hence, one expects the accuracy of the predictions to decline at lower TMP and at higher concentration of solids for a relatively low axial velocity (or TMP).

Another possible reason for the disagreement between measured filter flux and model predictions involves the term in the model describing the effect of axial velocity on filter flux. Many cross-flow filtration models predict filter flux to increase with increasing wall shear stress (i.e., increasing axial velocity). These models include boundary layer models, lift velocity models, and lateral migration models. The models described by equations 1 and 2 show the filtrate flux decreases with increasing axial velocity. In both instances, the terms describing the effect of axial velocity prove much smaller than the other terms in the models, and the coefficients in those terms prove smaller than their uncertainty. This axial velocity term causes the models to predict increases in filter flux with decreasing axial velocity, which will contribute to the difference observed between measured flux and predicted flux in this test. In addition, since the CUF contains 0.375" ID filter tubes and FRED contains 0.625" ID filter tubes, the wall shear stress in the CUF will exceed the wall shear stress in FRED at the same axial velocity, exaggerating this effect.

In addition to the mathematical analysis of the data set and equation, an equipment limitation likely contributed the deviation. During the engineering-scale filtration tests, high insoluble solids and low TMP produced a low filter flux. In many instances, the flux proved too low to measure with the instrumentation. For instance, Figure 4 and Figure 5 data for the Tank 8F sludge in the FRED include many flux values at the detection limit for the equipment.

Figure 12 shows a comparison of the current results with results of tests performed with the PREF using simulated waste. The PREF experiment involved a continuous concentration of sludge and MST from 1.15 g/L insoluble solids

to approximately 7 wt % insoluble solids. The results of the current test show good agreement with results from the test with the PREF. The overall standard deviation for the data from the PREF test equals ± 0.035 gpm/ft^2. The standard deviation for the tests using samples prepared with wet sludge equals ± 0.031 gpm/ft^2. The standard deviation for the tests using samples prepared with dry sludge equals ± 0.040 gpm/ft^2. The comparison also shows a positive bias for the experiment using slurry containing only Tank 51H sludge, a previously dried material.

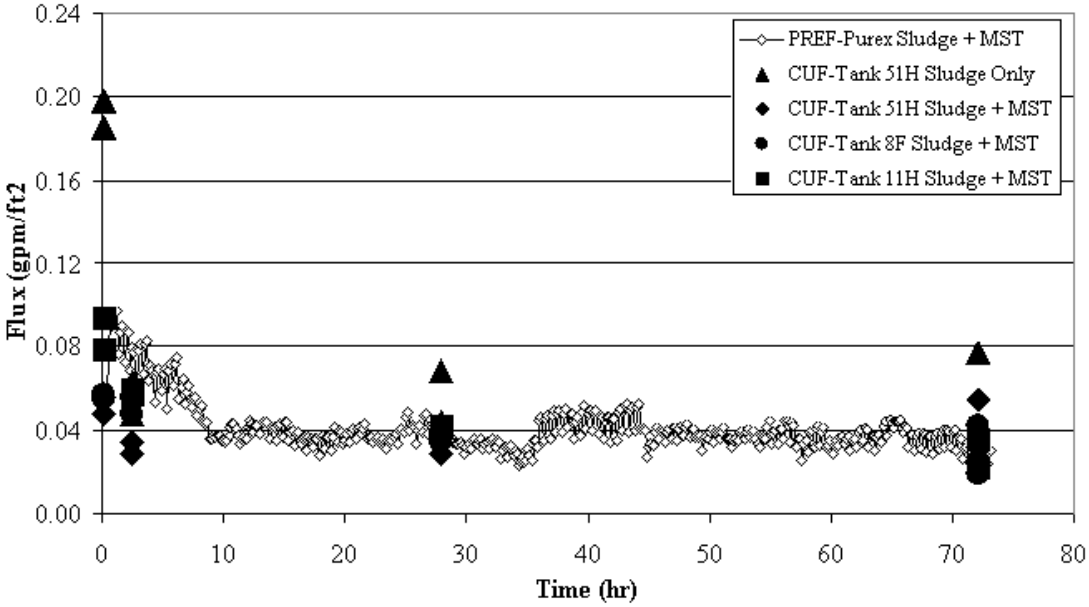

Figure 12. Comparison of Measured Flux for Similar Slurry Samples in CUF and PREF Equipment.

Table 4 in Appendix 1 shows the insoluble solids level and sodium concentration for each test. Table 5 in Appendix 1 shows the anion concentrations and supernate density for each feed stream. Table 6 in Appendix 1 shows results of previous analyses of the sludge solids.'

Thermal Analyses

The equipment used for the thermal analyses failed to calibrate correctly when tested with the indium standard. The equipment gave reproducible trends in the analyses but one can not accept the calculated heat capacities as reliable. Furthermore, personnel did not perform an analysis to determine the exact amount of solids or the ratio of MST to sludge in the samples. Hence, theses analyses only give qualitative insight into the behavior of the slurries.

Figure 13 displays the data from the calorimetry measurements. Each curve corresponds to a different sample. The figure shows the milliwatts of energy absorbed by the samples as a function of temperature. The measurements used sealed cups to hold the sample so evaporation had negligible influence on the results. As can be seen from Figure 13, the amount of energy absorbed by the samples (negative values on the ordinate) increased and reached a constant value with temperature. Energy absorption occurs due to the heat capacity of the sample. The heat capacity of a composite sample is the mass-weighted average of the heat capacity of each component. In this thermal test, the samples consist of the supernatant and solids. The solids include a mixture of sludge and MST. A closer look of Figure 13 reveals slurry samples from Tank 8F and 51H have slightly higher heat capacity than the corresponding sample using previously dried sludge. This may reflect structural changes in the sludge when it dries. For example, during drying gibbsite (aluminum hydroxide known to exist in wet sludge) converts to boehmite (aluminum oxide hydroxide). Boehmite has a lower heat capacity than gibbsite and this may account in part for the variance shown in the data. (A later report by Fondeur will address the structural changes of these sludge samples during drying.) Also, variance in the concentration of solids in the samples may also contribute to the observed differences in the measurements.

Previously, Taylor and Mattus observed a change in the rheology of slurries containing simulated sludge and MST when stored at 80 ° C for extended time. If a chemical reaction contributed to this change in rheology, one would expect to observe a thermal event at that temperature. Figure 13 does not contain noteworthy thermal events. The measurements by Taylor and Mattus occurred following a minimum storage period of one week. Future testing should include keeping the samples isothermal at 80 ° C (the temperature at which previous testing with simulated waste showed high yield points) for different length of times and then thermally ramping the samples for identification of thermal events.

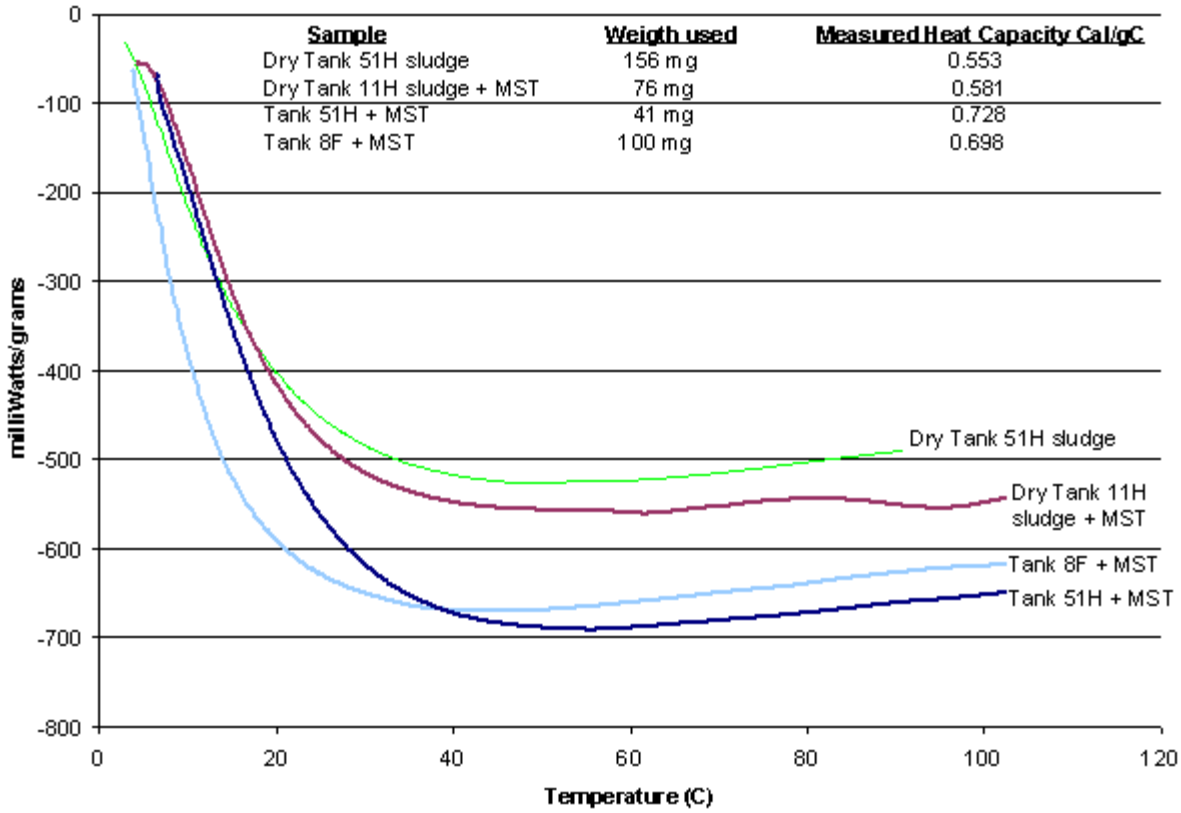

Figure 13. The Thermal Behavior of Dry and Wet Tank 51H and 8F Sludge With and Without MST.

Figure 14 displays the calorimetry data for similar experiments using slurry containing Tank 8F sludge and MST. In this experiment, sufficient sample existed to make the measurements for the individual slurries and for the composite. The curves for the Tank 8F sludge slurry and for the composite slurry – containing both Tank 8F sludge and MST -- overlap in the temperature range of 10 to 40 ° C. After 40 ° C the curve labeled "Tank 8F + MST" includes a broad endothermic peak which starts at 60 ° C. At present, we lack a definitive identification of the cause of the exothermic event. A similar peak started at an earlier temperature (40 ° C) in the experiment using the MST slurry. The shift in the temperature for this thermal event suggests an interaction of MST with the sludge. This peak did not reappear upon heating the same sample (i.e., Tank 8F sludge plus MST) indicating an irreversible process occurred.

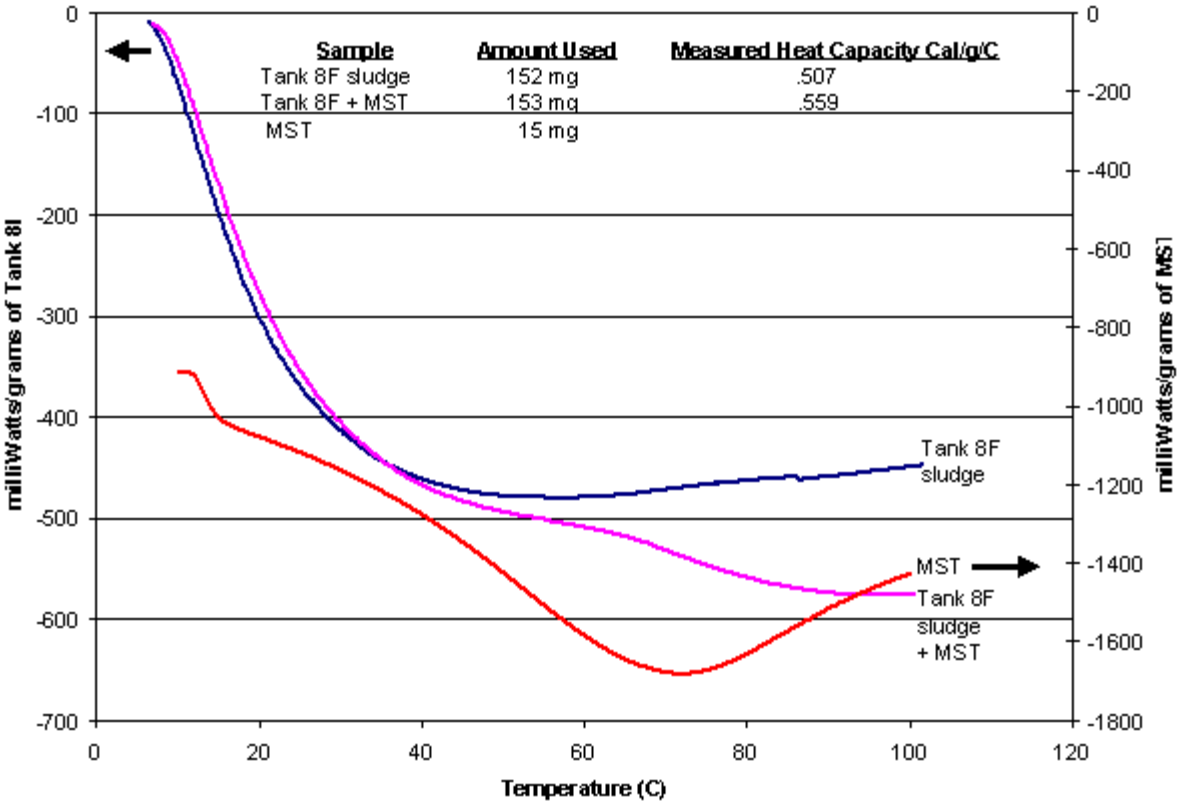

Figure 14 Thermal Behavior of Tank 8F Sludge With and Without MST.

Figure 15 provides additional calorimetry data for two experiments involving slurries containing Tank 51H sludge and a composite of Tank 51H sludge with MST. Note that the curve for the slurry containing both Tank 51H sludge and MST shows an early peak (near 20 ° C) that suggests the analysis occurred prior to achieving stable baseline conditions. Hence, the magnitude of the determined heat capacity for this test is not reliable.

One noticeable difference between the curves in Figure 15 involves the endothermic transition near 80 ° C due to MST. The same peak starts near 20 ° C in pure MST. This peak did not reappear upon heating the same sample, again indicating an irreversible process occurred.

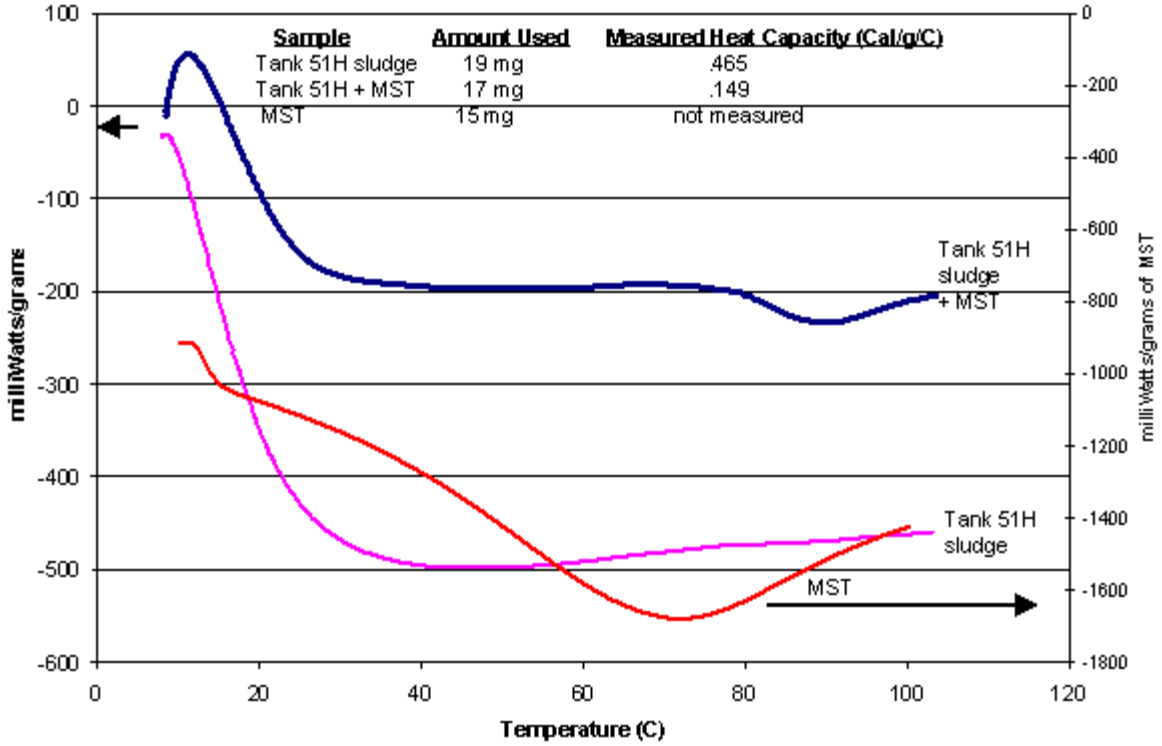

Figure 15 Thermal Behavior of Slurry Containing Tank 51H Sludge With and Without MST.

Figure 16 contains similar data for samples containing Tank 11H sludge and MST. Unlike the data for sludge from Tank 8F and Tank 51H, the curves indicate only a very minor endothermic event near 60 ° C after addition of MST. The variance of the energy for this endothermic event for the various composite samples indicates the degree of reaction differs for the different sludge compositions.

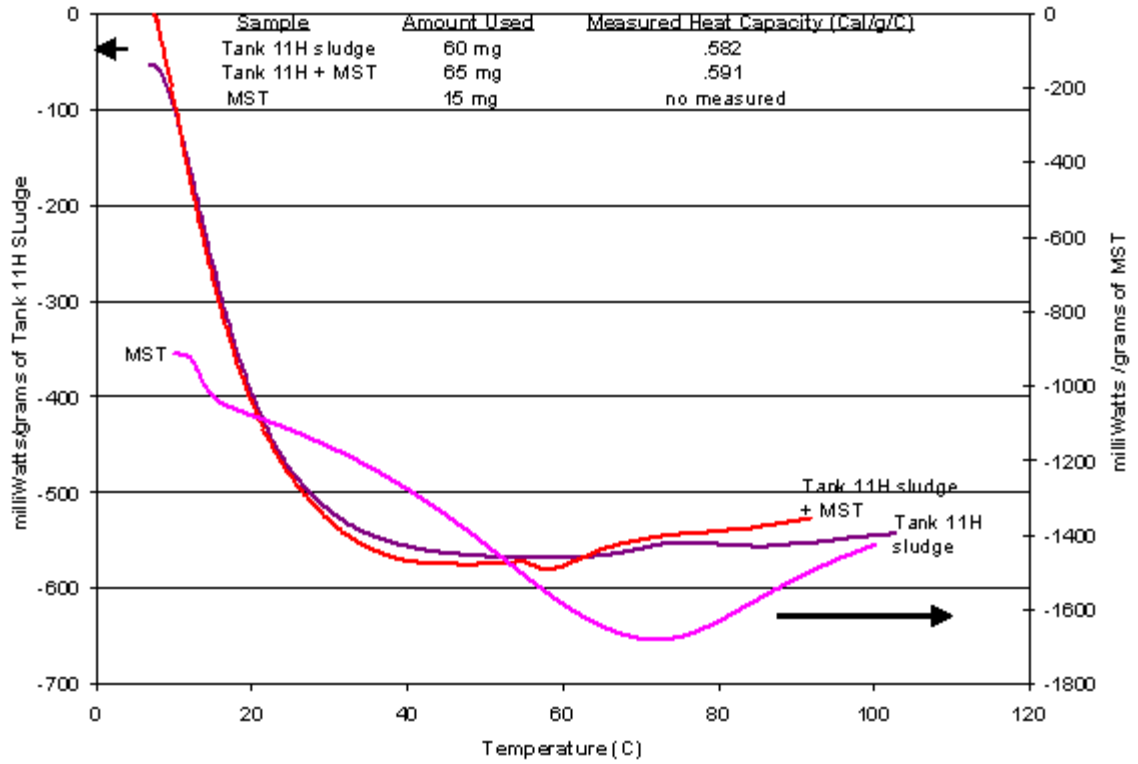

Figure 16. Thermal Behavior of Slurry

Containing Tank 11H Sludge With and Without MST.

Rheology Measurements

Appendix 3 contains plots of the data. Measurements occurred at 25 ° C. We regressed the uncorrected data obtained for all six samples using the Bingham Plastic model. We selected the Bingham plastic model because it provides a conservative yield stress measurement for these samples.

The Bingham plastic model is defined as:

$$Tau = Tau_o + \eta D \text{ or } \{ \tau = \tau_o + \eta\dot{\gamma} \}$$

Where:
Tau (τ) = Shear stress (Pa)
Tau_o (τ_o)= Shear stress at D = 0 s^{-1} (Pa)
η = consistency (cp)
D ($\dot{\gamma}$) = shear rate (s^{-1})

The regression used the rheological data generated from each sample over the shear rate range of $50s^{-1}$ to $1100s^{-1}$ except for sample containing Tank 8F sludge for which we evaluated the data over $50s^{-1}$ to $800s^{-1}$. Table 6 provides the Bingham Plastic model results for the samples along with previous rheology measurements with Tank 8F sludge. The rheological data from this test agrees reasonably well with the 1984 data.

Table 3. Bingham Plastic Model Results for the CUF Samples

Sample Name	Insoluble Solids	Yield Stress	Consistency	R^2
Tank 51H sludge	6.0 wt %	0.87 Pa	1.86 cp.	0.93
Tank 11H sludge plus MST	9.1 wt %	1.73 Pa	4.51 cp.	0.98
Tank 51H sludge plus MST	4.0 wt %	3.48 Pa	4.65 cp.	0.96
Tank 8F sludge plus MST	4.4 wt %	2.93 Pa	5.27 cp.	0.98
Tank 11H Sludge	6.0 wt %	0.83 Pa	5.78 cp.	0.97
Tank 8F Sludge	6.0 wt %	0.83 Pa	3.67 cp.	0.97
Tank 8F (1984)	5.4 wt %	0.9 Pa	3 cp.	N/A
Tank 8F (1984)	7.8 wt %	1.3 Pa	3 cp.	N/A
Tank 8F (1984)	8.3 wt %	1.3 Pa	4 cp.	N/A

N/A = not available

Conclusions

The conclusions from the testing follow.

- The filter flux for the real waste shows a positive bias relative to predictions based upon tests with simulated waste. The variance remains within the statistical accuracy of the predictive correlation except for slurries with the highest concentration of solids tested (i.e., 6.0 wt %)
- The simulated sludge used in previous cross flow filtration testing serves as a reasonable representative of actual

Savannah River Site sludge. Data from these tests provide a conservative estimate of equipment size and required operating conditions.
- We observed no significant difference in the filtration rates with Tank 51H sludge and Tank 8F sludge.
- Feed solutions prepared with dried sludge had higher filtration rates than feed solutions prepared with slurry sludge. Only a limited number of waste tanks contain dried sludge. Hence, the authors recommending using the behavior of the slurry samples as more representative of expected behavior for the process.
- The concentrated sludge and the sludge plus MST slurries (6.0 wt % insoluble solids) had yield stresses less than 3.5 Pa. The data agreed well with previous data where available.
- Thermal analysis shows a chemical reaction between MST and sludge at elevated temperatures (i.e., 60 – 80 °), possibly explaining the cause of previous observations of variance of rheology for such simulated waste slurries at these temperatures.

Quality Assurance

Laboratory Notebook WSRC-NB-2001-00034 (Poirier) contains filtration data and sample analyses for these experiments. The thermal analysis data resides in Laboratory Notebook WSRC-NB-99-00232 (P. U. Burkhalter). Fellinger recorded the rheology data in Laboratory Notebooks WSRC-NB-1999-00060, WSRC-NB-2000-00056, and WSRC-NB-2000-00165.

This work satisfies the requirements defined in the originating task plan as well as those defined in the feasibility study for this research. The work complied with "Procedure for Real Waste Test of The Small Tank Precipitation Process" (Manual L12.1, Procedure IWT-OP-137, Rev. 1) or earlier versions as appropriate. Check procedure title and revision

This report finalizes the work identified by Item 6.4 of "Applied Technology Integration Scope of Work Matrix for Alpha Removal (Demonstration Phase)," HLW-SDT-2000-00047, Rev. 3, November 9, 2000. The experiments using samples without MST addresses, in part, Item 6.5.3.

Acknowlegements

The authors thank the members of the various support groups that contributed to the success of this project. All members of the team worked many off-shift hours, including a large amount of uncompensated time, so as to complete the work in time for critical program decisions.

The Shielded Cells Operations staff ensured the success of the experiments through their tireless efforts. Maurice Lee, Denise Wheeler, Phyllis Burkhalter, Tim Allen, James Guthrie, Nan Stanley, and Richie Ryberg served as the operators for the filtration experiments. Bob Hartley also served as an operator and volunteered to shift assignments for the success of the program. Phyllis Burkhalter performed the thermal analyses. Maurice Lee and Jane Johnson performed the rheology measurements. Gary Hall repaired all the manipulators as needed on very short notice by working evenings and weekends. Babb Attaway, David Keel, Ron Blessing, and Carolyn Conley managed the extensive number of evolutions within the Shielded Cells in an incredibly smooth manner. Henry Bolton and Adrienne Williams prepared non-radioactive sample and materials needed for the test program. Henry Bolton performed the grinding operations to improve the particle size distribution of the MST.

Charles Nash and Hiroshi Saito assisted in preparing the equipment for operation. Dr. Saito provided technical assistance in performing some of the tests.

Steve Subosits served as the Process Engineering lead for the experiment. Lynn Nelson coordinated the efforts to issue the operating procedure. Bob Hinds chaired a readiness review for operations that helped focus the work.

The work benefited from the efforts of the talented staff that provided analytical support for the program.

References

1. H. H. Saito, M. R. Poirier, S. W. Rosencrance, and J. L. Siler, "Improving Filtration Rates of Mono-Sodium

Titanate (MST)-Treated Sludge Slurry with Chemical Additives", WSRC-TR-99-00343, September 15, 1999.
2. H. H. Saito, M. R. Poirier, and J. L. Siler, "Effect of Sludge Solids to Mono-Sodium Titanate (MST) Ratio on MST-Treated Sludge Slurry Cross-Flow Filtration Rates", WSRC-TR-99-00342, September 15, 1999.
3. Ralph Haggard, Travis Deal, Carol Stork, and Vince Van Brunt, "Final Report on the Crossflow Filter Testing for the Salt Disposition Alternative", USC-FRED-PSP-RPT-09-0-010, Rev. 0, December 4, 1998.
4. S. G. Subosits, HLWSDT-TTR-2000-00013, October 11, 2000.
5. M. R. Poirier, "FY2000 FRED Test Report,"WSRC-TR-2001-00035, Rev. 0, January 11, 2001 and included report "Final Report on the Crossflow Filter Optimization with 5.6 M Sodium Salt Solution" (V. Van Brunt, C. Stork, T. Deal, and R. Haggard, USC-FRED-PSP-RPT-09-0-015, December 20, 2000).
6. C. A. Nash, "Filtration of Tank 48H Contents with a Cells Unit Filter", WSRC-TR-95-0483, Rev. 0, December 8, 1995.
7. C. A. Nash, "Crossflow Filtration and Analysis of Tank 48H Post-December Contents", WSRC-TR-96-0112, Rev. 0, April 30, 1996.
8. C. A. Nash, H. H. Saito, and W. R. Wilmarth, "Strontium-Transuranic Precipitation and Crossflow Filtration of 241-AN-102 Large C", WSRC-TR-2000-00506, December 5, 2000.
9. V. Van Brunt, R. Haggard, T. Deal, C. Stork, M. R. Poirier, and S. D. Fink, "Cross-Flow Filtration of Simulated High-Level Waste Sludge (Tank 8F)", WSRC-TR-2001-00195, April 3, 2001.
10. A. L. Zydney and C. K. Colton, "A Concentration Polarization Model for the Filtrate Flux in Cross-Flow Microfiltration of Particulate Suspensions", Chem. Eng. Commun. Vol. 47, pp. 1 - 21, 1986.
11. M. S. Hay and N. E. Bibler, "The Characterization and Centrifuge-Settled Washing of a Tank 51H Sludge Sample Obtained in October 1995", WSRC-RP-95-1003.
12. T. L. Fellinger and N. E. Bibler, "Characterization of and Waste Acceptance Radionuclides to be Reported for DWPF Macro Batch 2 (ESP 215 -ESP 221)", WSRC-RP-99-00436, June 21, 1999.
13. R. F. Swingle, N. E. Bibler, and T. L. Fellinger, "Tank 8F Sludge Slurry Analysis Results", WSRC-RP-2000-00962, December 13, 2000.
14. D. T. Hobbs, M. J. Barnes, R. A. Peterson, and C. L. Crawford, "Radioactive Testin Results in Support of the In-Tank Precipitation Facility", WSRC-TR-98-00070, April 2, 1998.
15. K. Othmer, "Encylopedia of Chemical Technology, Fourth Edition," John Wiley & Sons, Volume 2, Page 319.
16. P. A. Taylor and C. H. Mattus, "Resuspension and Settling of Monosodium Titanate and Sludge in Supernate Simulant for the Savannah River Site," ORNL/TM-1999/166, September 1999.
17. B. A. Hamm, "High Level Caves Rheological Studies of Tanks 15H, 42H, and 8F Sludge/Slurries", DPST-84-439, April 11, 1984.
18. M. R. Poirier, "Task Technical and Quality Assurance Plan for the Real Waste Filtration Test," WSRC-RP-2000-00922, Rev. 1, February 21, 2001.
19. S.G. Subosits, "Feasibility Study - Cross-Flow Filtration Testing with Real High Level Waste", HLW-SDT-2000-00415, Rev. 0, October 9, 2000.

Appendix 1. Analytical Data

Table 4. Analysis of Sodium and Insoluble Solids in Feed Solutions

Feed Solution	Target Insoluble Solids Level (wt %)	Measured Insoluble Solids (wt %)	Na by AA (M)	Na by ICP-ES (M)
Tank 51H Sludge Only	0.06	< 0.03	4.2	5.6
Tank 51H Sludge Only	0.29	0.087	2.9	3.9
Tank 51H Sludge Only	1.29	0.289	3.9	4.5
Tank 51H Sludge Only	6.0	*	3.8	4.9
Tank 51H Sludge + MST	0.06	< 0.03	3.6	4.7
Tank 51H Sludge + MST	0.29	006	6.9	6.7

Tank 51H Sludge + MST	1.29	0.97	3.9	5.2
Tank 51H Sludge + MST	6.0	4.0	3.5	4.2
Tank 8F Sludge + MST	0.06	0.26	5.2	4.9
Tank 8F Sludge + MST	0.29	0.29	9.8	9.8
Tank 8F Sludge + MST	1.29	0.59	5.3	5.8
Tank 8F Sludge + MST	6.0	4.35	3.7	5.0
Tank 11H Sludge + MST	0.06	0.203	1.8	2.1
Tank 11H Sludge + MST	0.29	0.473	4.9	4.6
Tank 11H Sludge + MST	1.29	0.936	3.4	4.1
Tank 11H Sludge + MST	6.0	9.12	4.1	3.9

Result not received.

Table 5. Analysis of Feed Supernatant

Species	Tank 51H Sludge Only	Tank 51H Sludge + MST	Tank 8F Sludge + MST	Tank 11H Sludge + MST
OH	10.9 M	*	*	*
NO2	0.73 M	0.33 M	0.39 M	0.33 M
NO3	0.84 M	0.45 M	0.46 M	0.37 M
AlO2	0.14 M	0.14 M	0.19 M	0.11 M
SO4	n.d.	n.d.	n.d.	n.d.
Cl	n.d.	0.003 M	0.003 M	0.003 M
F	n.d.	n.d.	n.d.	n.d.
PO4	n.d.	n.d.	n.d.	n.d.
oxalate	n.d.	n.d.	0.01 M	0.01 M
density	1.227 g/mL	1.215 g/mL	1.201 g/mL	1.218 g/mL

*** Result not received.**
n.d. species not detected

Table 6. Analysis of Sludge Used in Real Waste Filter Tests

Species	Tank 51H Dried Sludge (wt %)	Tank 51H Slurry Sludge (wt %)	Tank 8F Slurry Sludge (wt %)	Tank 11H Dried Sludge (wt %)
Ag		0.019	0.015	0.21
Al	5.6	7.7	3.9	24.6

B		0.0055	< 0.006	
Ba		0.046	0.023	0.16
Ca	2.2	2.2	0.86	0.86
Cd		0.11	0.0062	0.064
Cr	0.16	0.13	0.16	0.25
Cu	0.024	0.030	0.033	0.26
Co		0.0076	0.0099	
Fe	22.1	21.5	21.5	11.0
Hg	0.14	0.86	0.12	4.04
K		< 0.05	-	
La		0.021	0.018	0.36
Li		0.0066	0.063	0.14
Mg	1.1	1.2	0.57	0.13
Mn	2.3	3.3	1.8	5.8
Mo		0.0046	< 0.008	0.060
Na	14.4	5.8	23.5	9.4
Ni	0.27	0.34	1.0	2.3
P	0.48	0.66	0.23	0.32
Pb		0.075	0.037	0.56
Si	0.57	1.3	0.56	0.88
Sn		0.0096	< 0.02	0.086
Sr		0.019	0.012	0.031
Ti	0.013	0.017	0.029	0.095
U	3.1			
V		0.0078	0.008	0.22
Zn		0.0036	0.028	0.13
Zr		0.021	0.052	

Appendix 2: Rheology Equipment Details and Control Standard

The technical specifications for the RV30/M5 system are listed in Table 7.

Table 7. Technical Specifications for the System

(Date taken from "Haake, "Instruction Manual Rotovisco RV30".)

Speed Range:	5E-02 to 5E02 rpm
Shear Rate Range:	4E-03 to 4E04 s^{-1}
Shear Stress Range:	2E-01 to 7E04 Pa
Viscosity Range:	5E00 to 1E09 mPa
Temperature Range:	Depends on Water Bath /Circulator
Maximum Torque:	4.9 Ncm
Minimum Torque:	0.049 Ncm

The error in the measured shear stress is 0.5% of full span (100%Tau) and the error for the measured shear rate is 0.5% of the reading. Table 8 provides the maximum shear rate, maximum shear stress, and physical dimensions associated with MV1 rotor.

Table 8. Maximum Shear Rate, Maximum Shear Stress, and Physical Dimensions Associated with the MV1 Rotor

(Date taken from "Haake, "Instruction Manual Rotovisco RV30".)

MV1 Rotor – Maximum Tau (Pa) and D (1/s)

100% Tau = 322 Pa
100% D = 1170 (1/s)

MV1 Rotor – Physical Dimensions

Inner Cylinder (Rotor)
- Radius R_i – 20.04 mm
- Height L – 60 mm

Outer Cylinder (Cup)
- Radius R_a – 21 mm

Radii Ratio (R_a/ R_i) – 1.05
Gap Width – 0.96 mm
CI factor (Torque correction factor which incorporates rotor end effects) – 1.0053*

*WSRC-NB-2000-00165

Programming of the RV-30

We selected different programming times and shear rate ranges based on the visual observations of the samples. Table 9 contains the different programming times and shear rate ranges for the six samples.

Table 9. Programming Times and Shear Rate Ranges Selected for the Slurry Samples

	Tank 51H Sludge	**Tank 11H Sludge plus MST**	**Tank 51H Sludge plus MST**	**Tank 8F Sludge plus MST**	**Tank 11H Sludge**	**Tank 8F Sludge**
Shear Rate Range and						

Time for the Up Curve	0 - 1100s^{-1}, 4 minutes	0 - 1100s^{-1}, 5 minutes	0 - 800s^{-1}, 5 minutes	0 - 1100s^{-1}, 5 minutes	0 - 1100s^{-1}, 5 minutes	0 - 1100s^{-1}, 5 minutes
Shear Rate Range and Time for the Down Curve	1100 - 0s^{-1}, 4 minutes	1100 - 0s^{-1}, 5 minutes	800 - 0s^{-1}, 5 minutes	1100 - 0s^{-1}, 5 minutes	1100 - 0s^{-1}, 5 minutes	1100 - 0s^{-1}, 5 minutes

Figure 17 contains the response curve for the control standard.

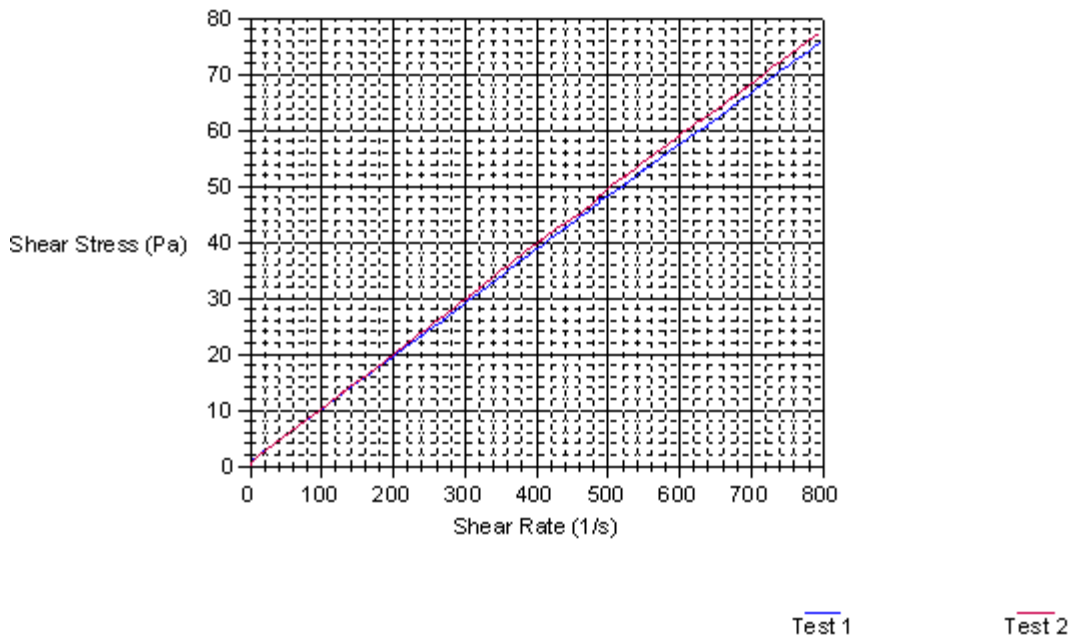

* Note - Data below or at 3.22 Pa on the Y Axis is in the 1% region for Tau. Data in the 1% region could have errors of ± 50%. The MVI rotor was used for this measurement.

Figure 17. Up Flow Curves for the Newtonian Oil Standard

As shown in the following table, the measurements for the control standard agreed well with the expected values.

Test Number	Model Used To Fit Data	Known Consistency	Consistency Measured	R^2 Fit
Test 1	Newtonian	95.6 cp	96.6 cp	1.00
Test 2	Newtonian	95.6 cp	98.9 cp	1.00

Appendix 3: Rheology Data and Figures

Figure 17 through Figure 23 contain the raw data obtained from the rheometer (up flow curves only). Measurements occurred at 25 ° C. Figure 24 compares the data for slurry samples containing Tank 51H sludge with and without MST. Figure 25 compares the data for the slurry samples containing Tank 8F sludge with and without MST. Figure 26 compares the data for the slurry samples containing Tank 11H sludge with and without MST. We chose to omit the measurements of the down flow curves and obtain the fluid property values from the up flow curves.

We measured multiple flow curves for each sample. These flow curves proved repeatable, since they overlaid each other. Also the viscosity determined for the Newtonian oil standard remained within 5% of its known value, indicating that the instrument performed as expected.

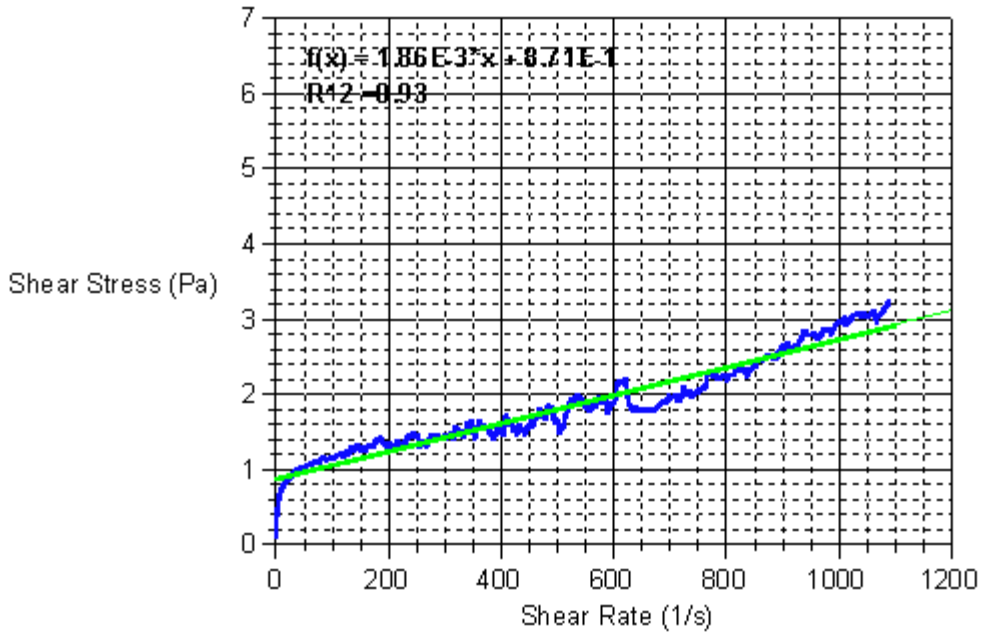

* Note - Data below or at 3.22 Pa on the Y Axis is in the 1% region for Tau. Data in the 1% region could have errors in excess of ± 50%. The MVI rotor was used for this measurement.

Figure 18. Uncorrected Flow Curve for Tank 51H Sludge Slurry Sample

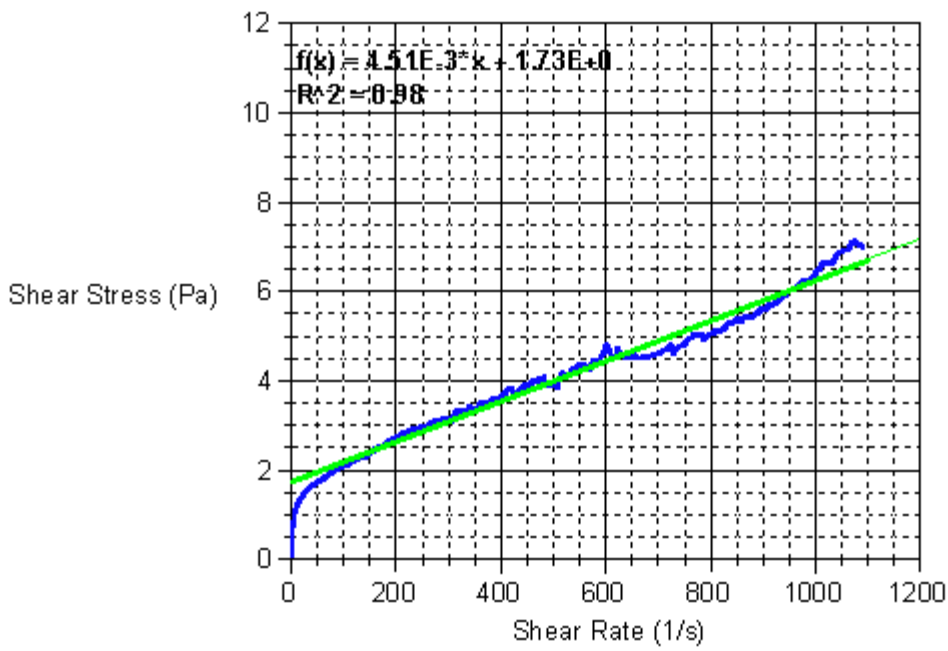

* Note - Data below or at 3.22 Pa on the Y Axis is in the 1% region for Tau. Data in the 1% region could have errors in excess of ± 50%. The MVI rotor was used for this measurement.

Figure 19. Uncorrected Flow Curve for Sample Containing Tank 11H Sludge Plus MST

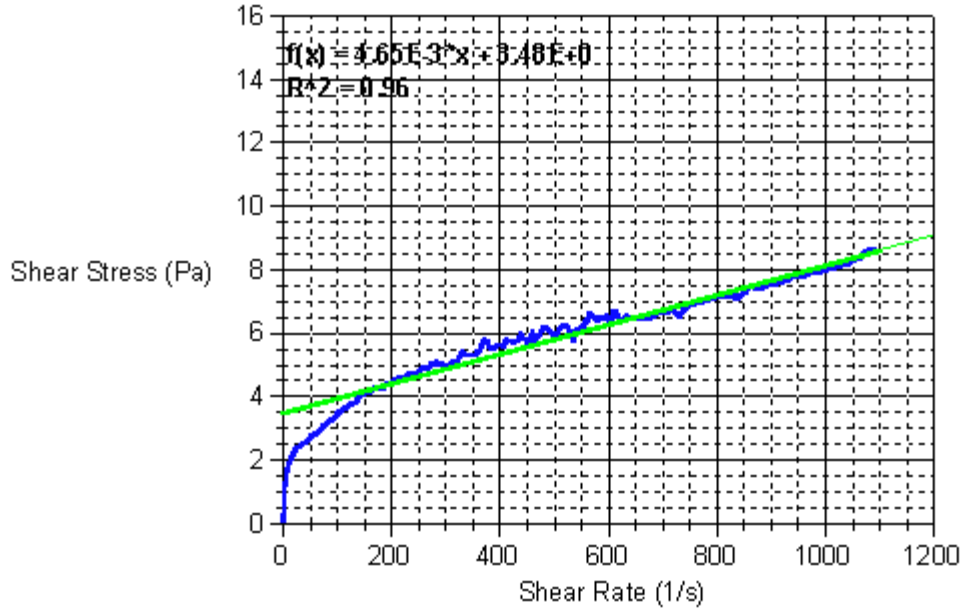

* Note - Data below or at 3.22 Pa on the Y Axis is in the 1% region for Tau. Data in the 1% region could have errors in excess of ± 50%. The MVI rotor was used for this measurement.

Figure 20. Uncorrected Flow Curve for Sample Containing Tank 51H Sludge Plus MST

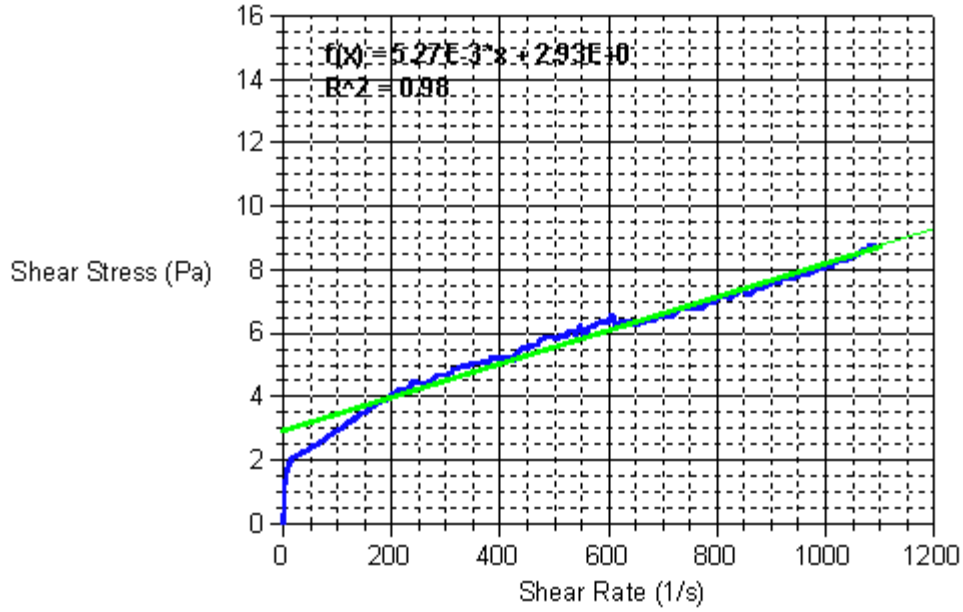

* Note - Data below or at 3.22 Pa on the Y Axis is in the 1% region for Tau. Data in the 1% region could have errors in excess of ± 50%. The MVI rotor was used for this measurement.

Figure 21. Uncorrected Flow Curve for Sample Containing Tank 8F Sludge Plus MST

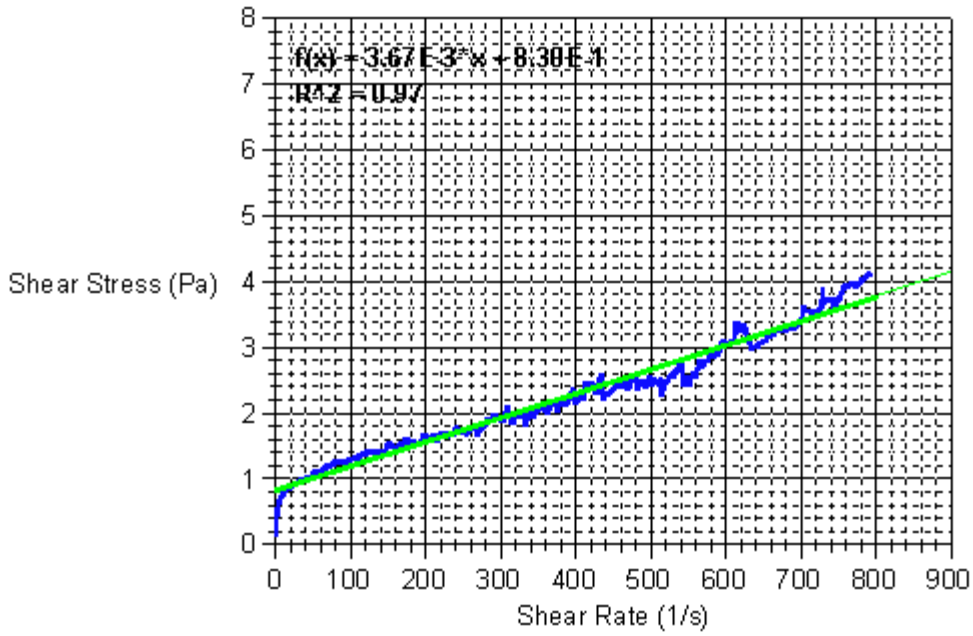

* Note - Data below or at 3.22 Pa on the Y Axis is in the 1% region for Tau. Data in the 1% region could have errors in excess of ± 50%. The MVI rotor was used for this measurement.

Figure 22. Uncorrected Rheology Flow Curve for Tank 8F Sludge Slurry Sample

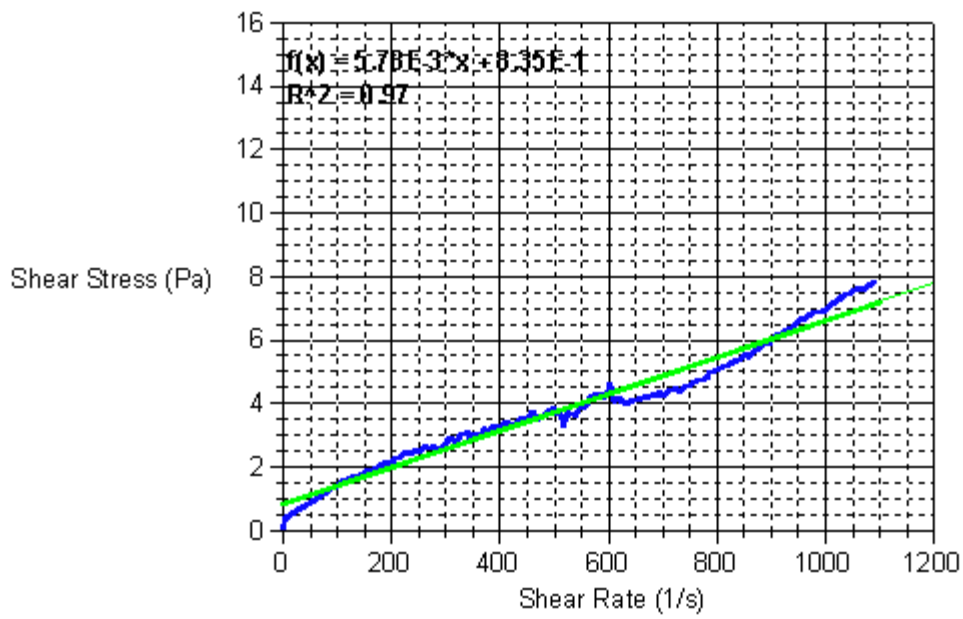

* Note - Data below or at 3.22 Pa on the Y Axis is in the 1% region for Tau. Data in the 1% region could have errors in excess of ± 50%. The MVI rotor was used for this measurement.

Figure 23. Uncorrected Rheology Flow Curve for Tank 11H Sludge Slurry Sample

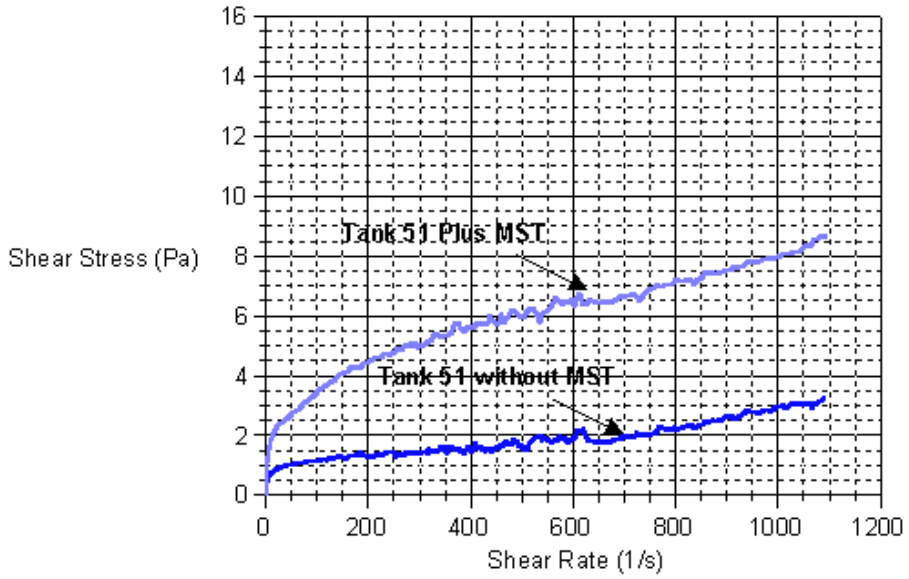

* Note - Data below or at 3.22 Pa on the Y Axis is in the 1% region for Tau. Data in the 1% region could have errors in excess of ± 50%. The MVI rotor was used for this measurement.

Figure 24. Comparison of the Uncorrected Flow Curves for Samples Containing Tank 51H Sludge and Containing Tank 51H Sludge Plus MST

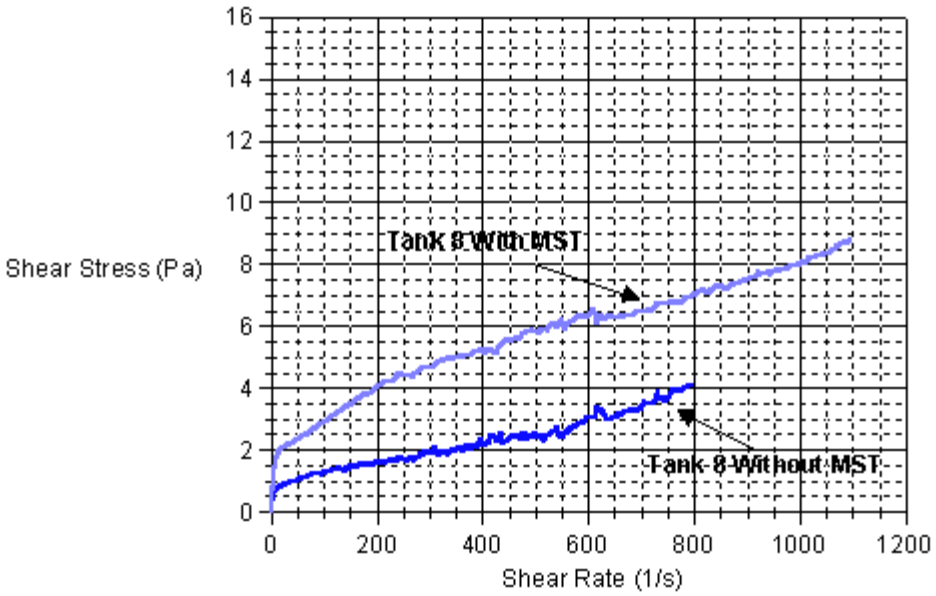

* Note - Data below or at 3.22 Pa on the Y Axis is in the 1% region for Tau. Data in the 1% region could have errors in excess of ± 50%. The MVI rotor was used for this measurement.

Figure 25. Comparison of the Uncorrected Rheology Flow Curves for Samples Containing Tank 8F Sludge and Containing Tank 8F Sludge Plus MST

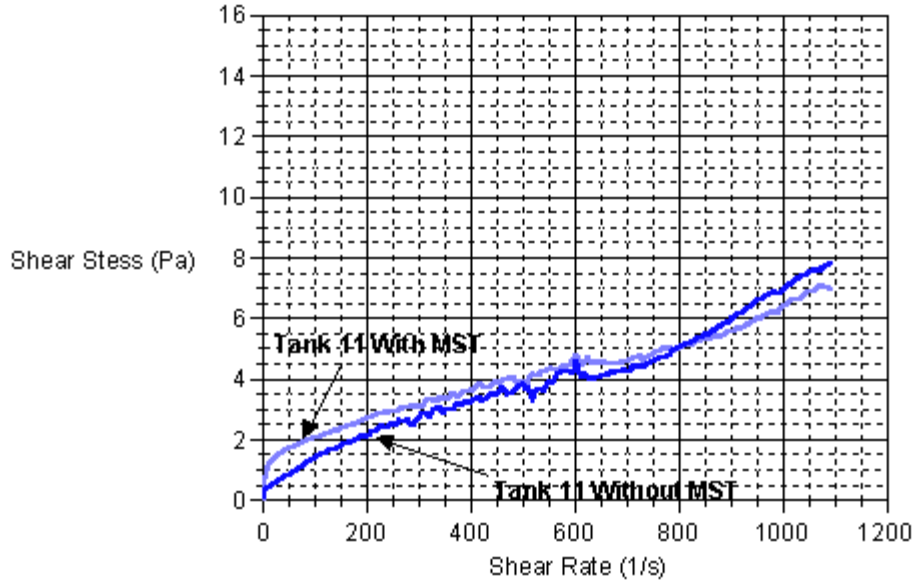

* Note - Data below or at 3.22 Pa on the Y Axis is in the 1% region for Tau. Data in the 1% region could have errors in excess of ± 50%. The MVI rotor was used for this measurement.

Figure 26. Comparison of the Uncorrected Rheology Flow Curves for Samples Containing Tank 11H Sludge and Containing Tank 11H Sludge Plus MST